Building Electro-Optical Systems
Corrected Figures

Philip C. D. Hobbs

Version 2.5
December 10, 2003

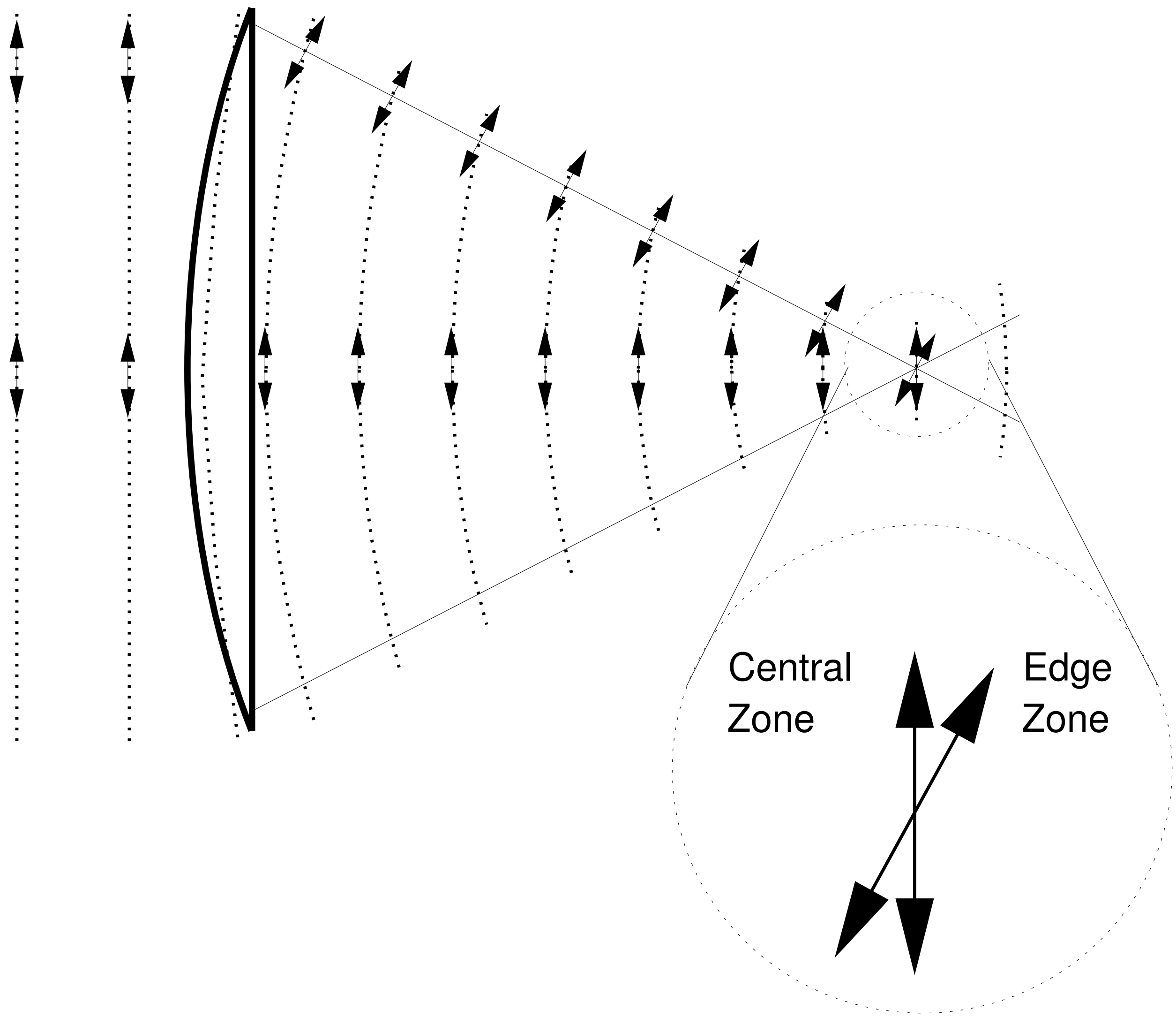

Figure 1.2 Scalar addition is a reasonable approximation to vector addition except near high-NA foci and caustics. Near focus, there are longitudinal field components and a reduced phase derivative with respect to z ($|\Delta\phi| < |k\Delta z|$.

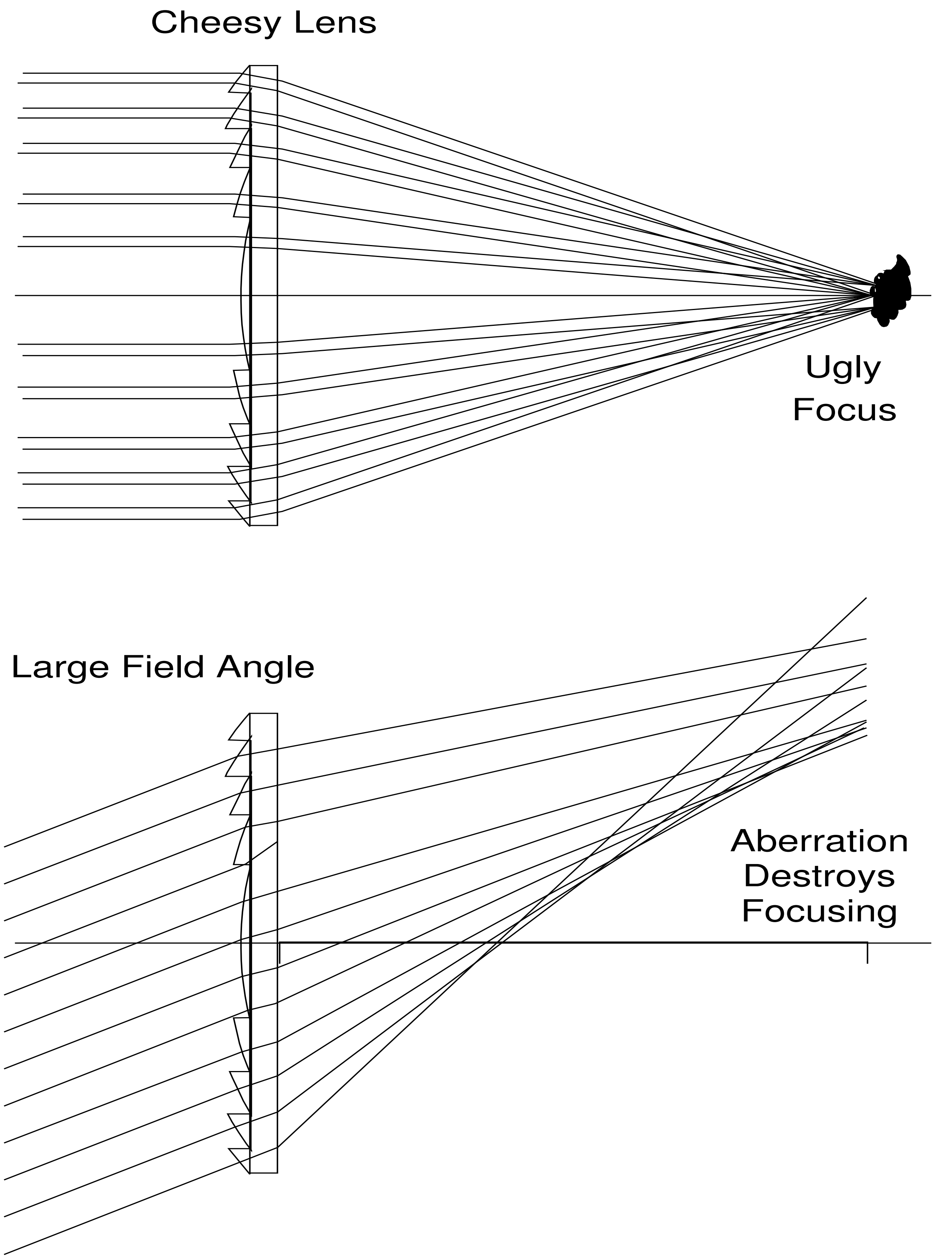

Figure 4.9 The Fresnel lens: A great idea for very low-performance and highly cost-sensitive applications, such as condensers and IR motion detectors.

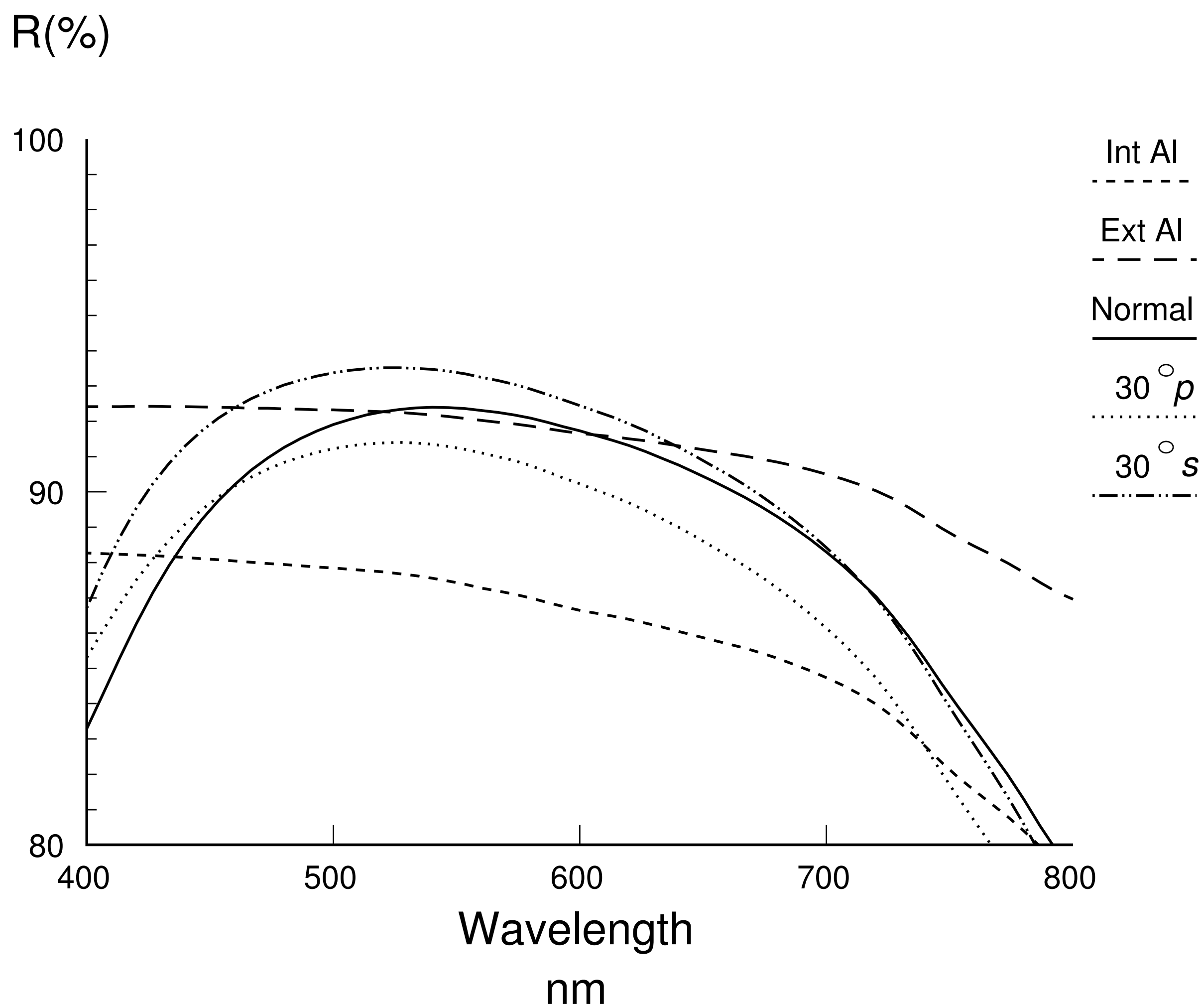

Figure 5.6 The protected aluminum mirror: 0.5 wave @520nm of SiO (1.7) over Al.

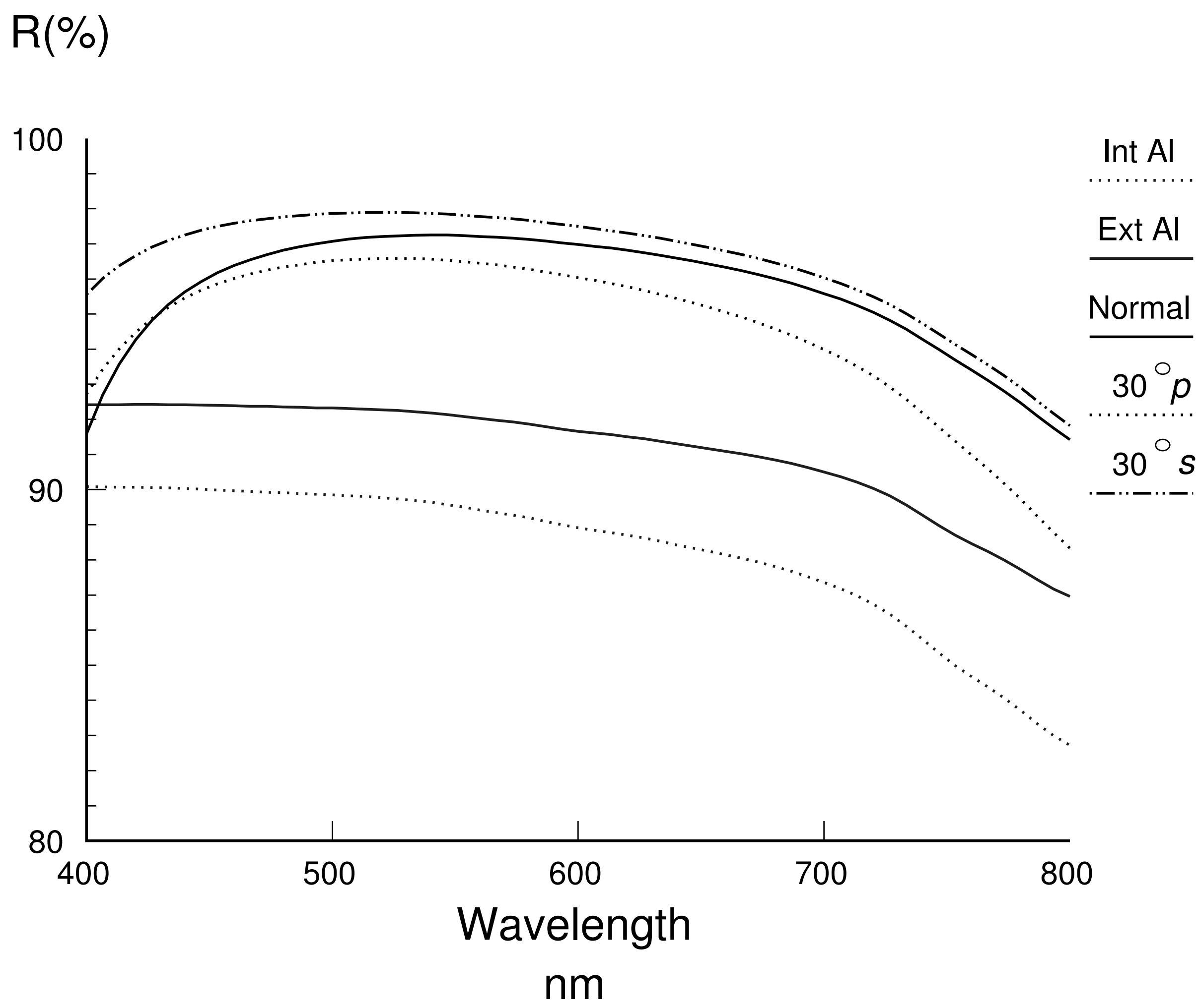

Figure 5.9 Replacing the 0.5 wave of SiO with 0.25 waves each of ZnS over MgF_2 yields a substantially improved metal mirror for the visible, the enhanced aluminum coating.

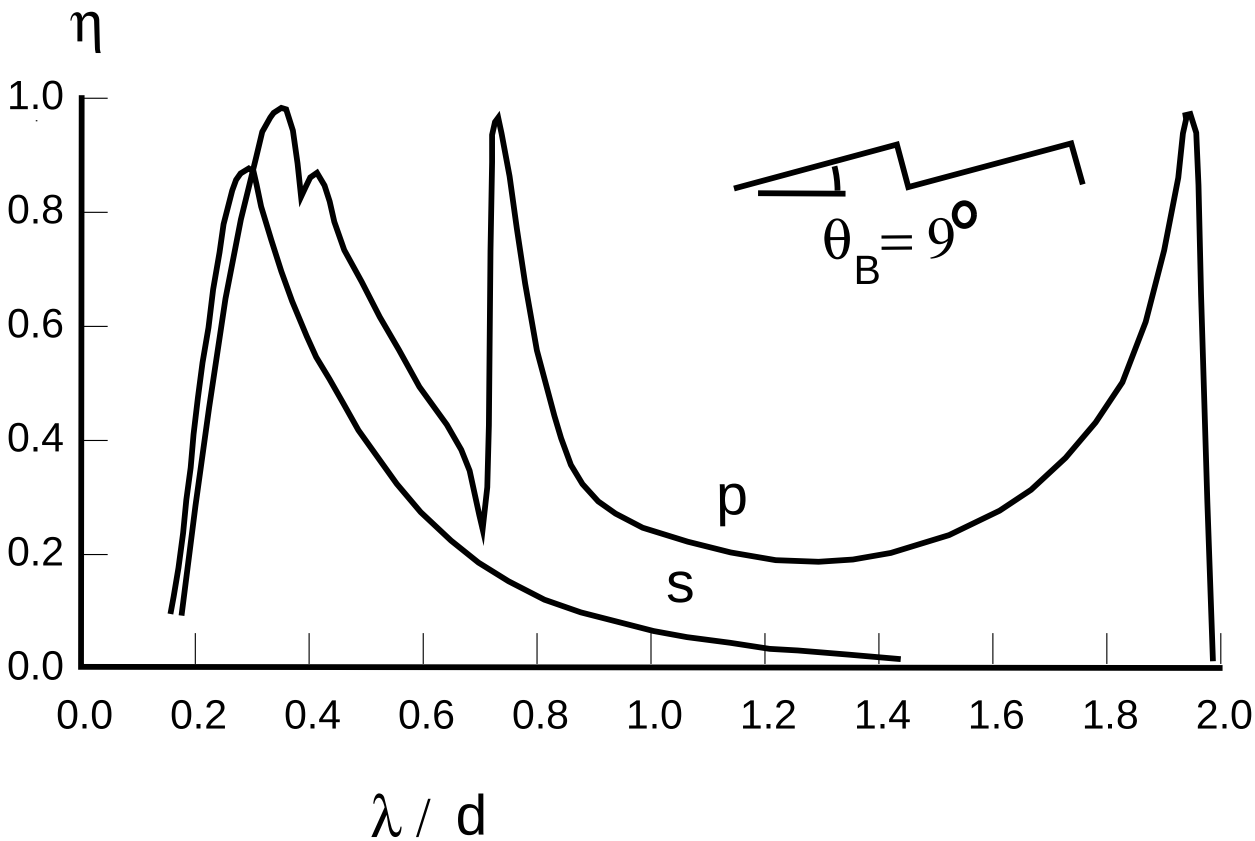

Figure 7.6: Theoretical diffraction efficiency in Littrow of a 9° blazed ruled grating. Note the strong Wood's anomalies and polarization dependence. Figure courtesy of The Richardson Grating Laboratory.

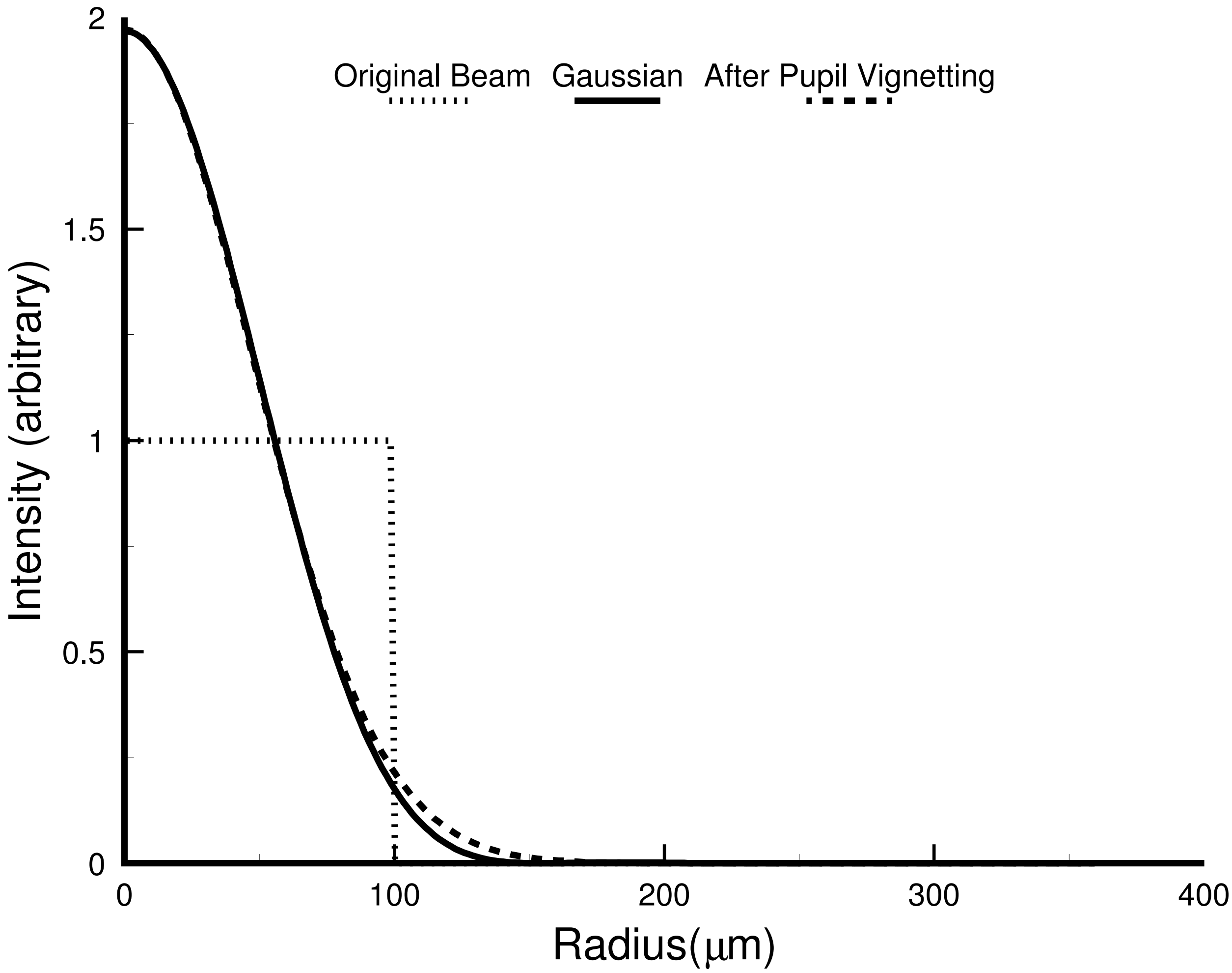

Figure 9.13: Turning a uniform beam into a nearly-Gaussian beam, using a circular spatial filter of the same radius as the first Airy null.

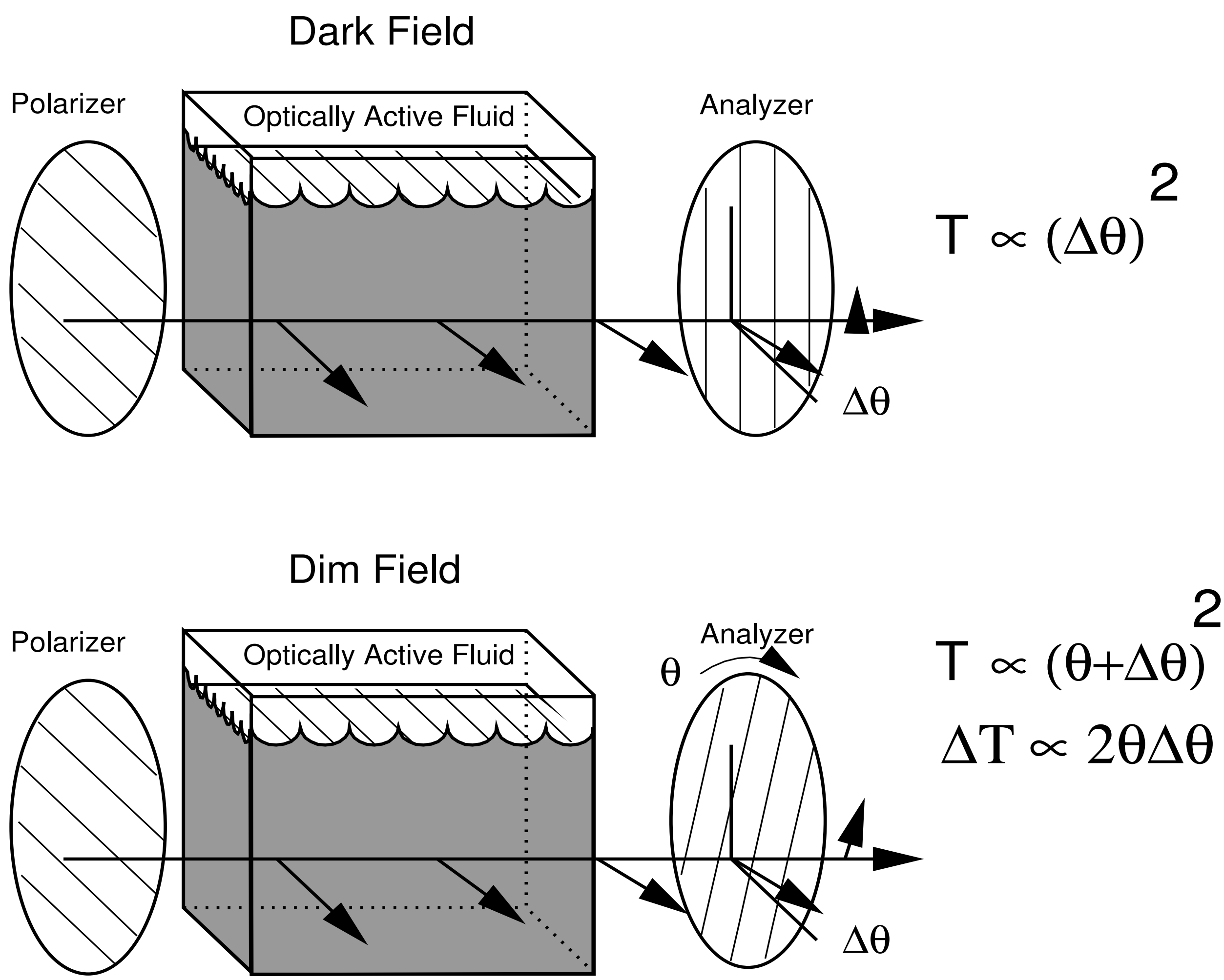

Figure 10.2: Dim field measurements use a bit of coherent background as an LO signal. Here a crossed-polarizer measurement gets a SNR boost from uncrossing them a bit.

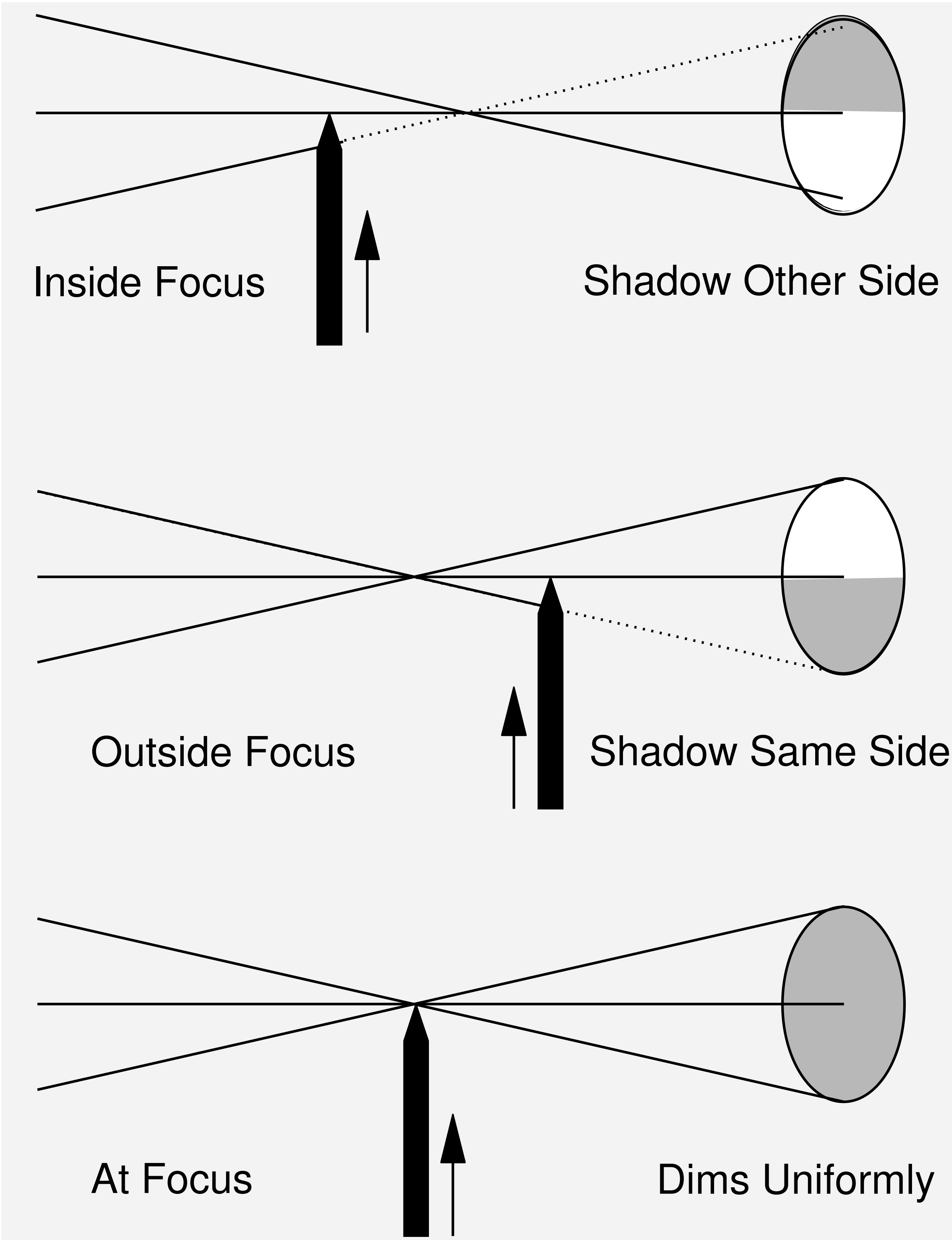

Figure 12.2: Knife edge test

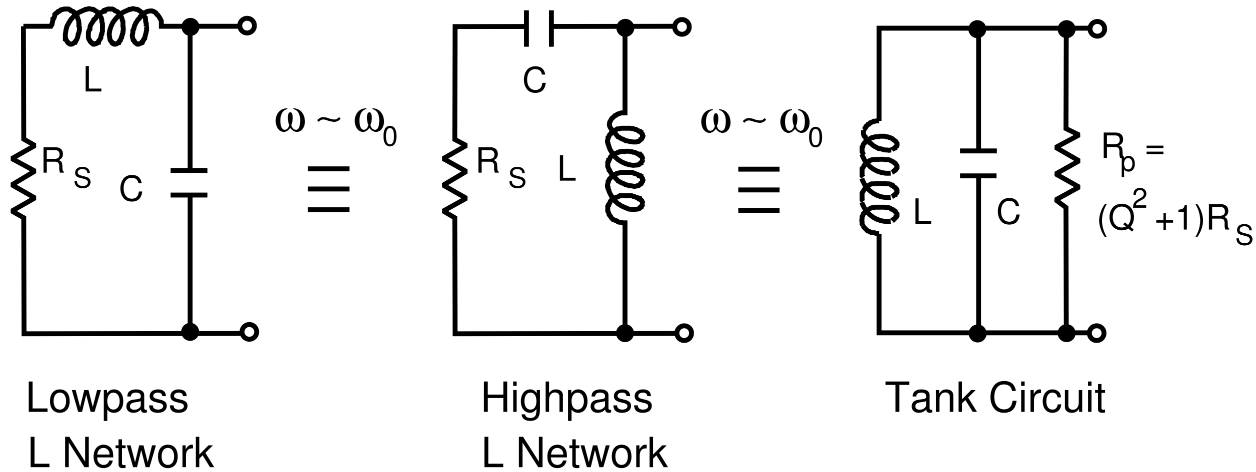

Figure 14.4: In the high-Q limit (Q >≈ 5), near resonance, an L-network multiplies R_s by Q^2+1 to get equivalent R_p. The three forms have very different skirt selectivity.

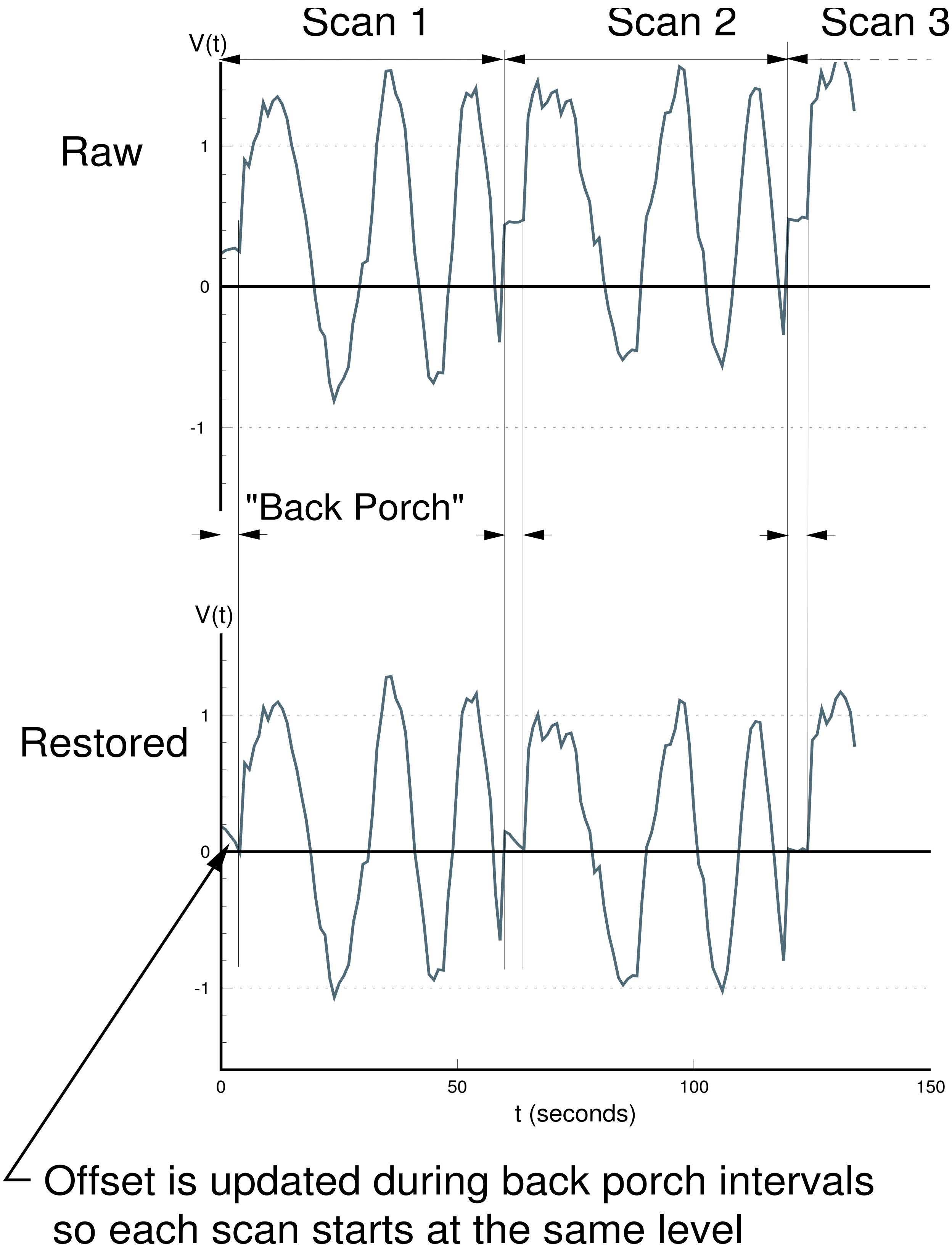

Figure 17.1: Baseline restoration works well when the signal drift is sufficiently slow and uniform across the scan that a single correction point per scan line is enough.

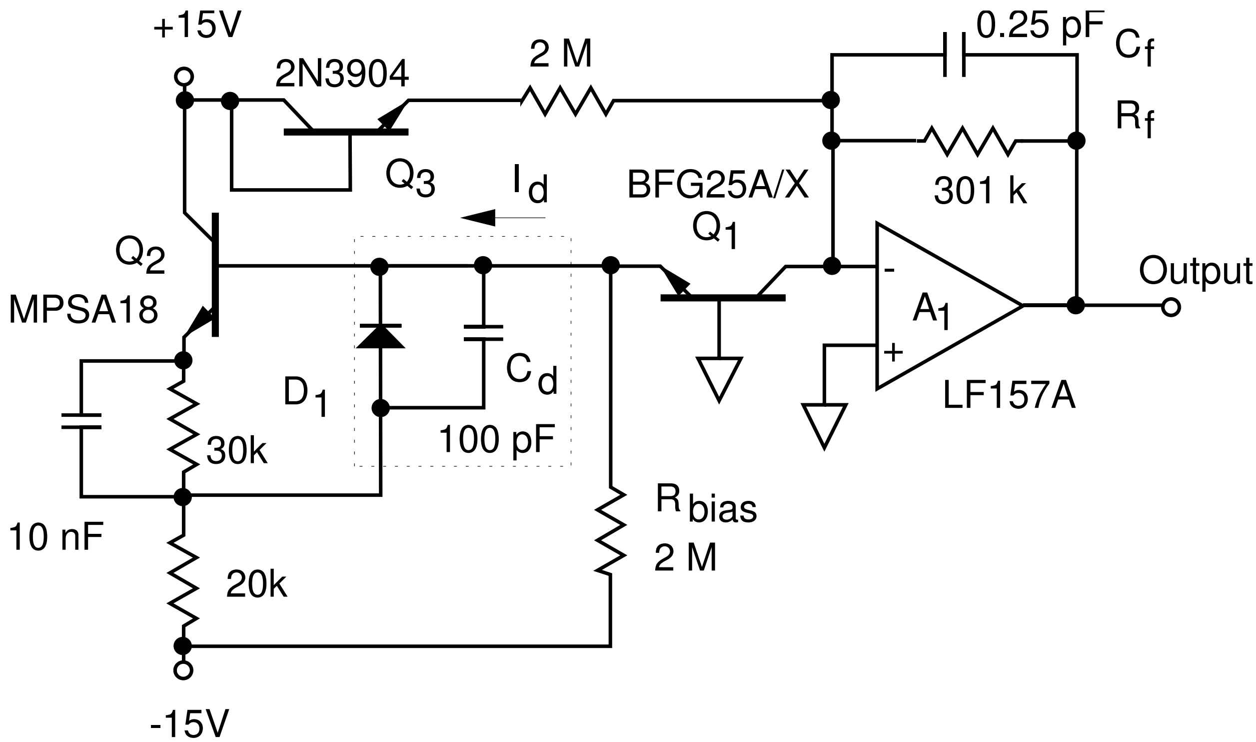

Figure 18.14 Final circuit: cascode Q_1 plus bootstrap Q_2 cope with the obese 100 pF diode; Q_3 corrects for V_{be} of Q_1 (300 µV/°C at the output).